

# A NOVEL APPROACH FOR OPTIMALLY MATCHING A LATE REVERBERATION MODEL TO AN IMAGE SOURCE MODEL - OR: WHAT DOES A FOOTBALL HAVE TO DO WITH SHOEBOX SHAPED ROOMS?

Christian Borß

Institute of Communication Acoustics  
Ruhr-Universität Bochum  
Bochum, Germany  
christian.borss@rub.de

## ABSTRACT

For the synthesis of virtual acoustics it is common practice to simulate early reflections and late reverberation by different rendering models, e.g., an image source model for the early reflections and a statistical model for the late reverberation. A binaural room impulse response synthesized by the late reverberation model can be smoothly combined with the early reflections by applying a fade-in function. In this paper we present a new algorithm for “shoebox” room geometries which derives such a fade-in function directly from the parameters of the image source model.

## 1. INTRODUCTION

Real-time modeling of room acoustics is used in diverse fields of applications, e.g., for pure entertainment purposes in computer games or for predicting room acoustics in the field of architectural acoustics. While a perceptual approach [1, 2, 3] is appropriate for the former example, the latter requires a physical approach [4]. Ray-tracing techniques [5] or variants like beam-tracing [6] or cone-tracing [7] allow for an efficient simulation of high-order reflections. Such techniques are frequently used in physically-based auralization software [8, 9, 10, 11, 12]. They can be further extended to also incorporate portions of diffuse reflections [13, 14]. Hybrid models distinguish between early and late reflections, e.g. by using an image source method [15] to yield deterministic early reflections [16].

Due to the diffuse character of the late reverberation, artificial reverberators are used in perceptual approaches for modeling late reverberation [17, 18]. Artificial reverberators constructed from all-pass filters and comb filters [19, 20, 21, 22] or feedback-delay networks [23] are frequently combined with the early reflection rendering module by a serial connection [1, 2, 21, 22]. Since the computational load of a convolution with a room impulse response is no longer a restriction for a real-time implementation on a current PC [24], convolution-based reverberators can be a good alternative for a state-of-the-art auralization software. Statistical time-frequency models which use a random noise signal and a filterbank for the synthesis of an artificial reverberation tail [20] can completely avoid the coloration which can be observed for not properly tuned filter networks [25].

As the determination of the propagation paths and the involved reflections are part of the ray-/beam-/cone-tracing algorithm, it can easily be combined in a hybrid physical approach with an image source model. In a hybrid perceptual approach where an image source model is used together with an artificial reverberation

model, a strategy for the combination has to be found. This can be done by adding the late reverberation after a certain amount of time, e.g. by using a single delay in the case of a feedback-delay network or by using a fade-in function for a synthesized impulse response. As 80-100 ms have been found in psycho-acoustical investigations as the point where the late reverberation starts [26, 27], this would be a proper choice for the delay. However, it would be desirable if the combination strategy could be derived from the model as it is the case in the physically-based hybrid model.

In this paper we focus on hybrid perceptual approaches which simulate specular reflections based on physical principles. Further details about our implemented software (“*tinyAVE*”) and an explanation how we generate early reflections and late reverberation with a matching timbre can be found in [3]. Examples for a proper choice of the rendering parameters like, e.g., the frequency dependent reverberation time are given in [24]. Audio examples can be found in [28].

## 2. COMBINATION OF EARLY AND LATE REVERBERATION MODELS

A shoebox room results in a regular pattern of image sources where each image source belongs to a certain *image source room*. These image source rooms are mirrored versions of the simulated room. If an image source model simulates early specular reflections up to a certain order, the corresponding image source rooms form to-

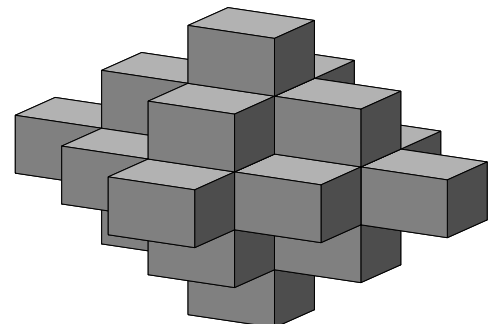


Figure 1: Geometrical structure which results from all image source rooms up to the second order for a shoebox geometry

gether a space which is covered by the model. An example for this joined image source space resulting from all image source rooms up to the second order is shown in Fig. 1.

The basic idea of our algorithm is that we can yield perfectly matched early and late reverberation rendering models if the late reverberation model covers the space which is not covered by the image source model. Figure 2 shows a cross section of the image source space shown in Fig. 1 to illustrate this idea. The crosses in this figure mark the image sources which result from the sound source, marked by a bold cross, in the simulated shoebox room. The corresponding image source rooms are indicated by the white areas. The gray area marks the space which is not covered by the image source model and thus has to be covered by the late reverberation model. For a receiver located in the center of the room, the two circles with radius  $r$  and  $r + dr$  indicate the spherical shell which contributes to the room impulse response  $h(t)$  in the infinitesimal short time period  $t \dots t + \frac{dr}{c}$ , where  $c$  denotes the speed of sound. The volume  $V(ct) = A(ct)dr$  of this infinitesimal thin spherical shell consists of two parts, the volume  $V_m(ct) = A_m(ct)dr$  which belongs to the image source model and the volume  $V_l(ct) = A_l(ct)dr$  which belongs to the late reverberation model.

The ratio  $\frac{V_l(ct)}{V(ct)} = \frac{A_l(ct)}{A(ct)}$  contains the information about the optimally matched contribution of the late reverberation model to the room impulse response  $h(t)$  in the infinitesimal short time period  $t \dots t + \frac{dr}{c}$ . We therefore propose to match the rendering models by using the ratio  $\frac{A_l(ct)}{A(ct)} = 1 - \frac{A_m(ct)}{A(ct)}$ . This can be implemented by adjusting

- a) the intensity profile or
- b) the echo density profile

of the late reverberation tail. Figure 3 shows an example for the area  $A_m(ct)$  of the intersection surface which may remind the reader of a *football*<sup>1</sup>. This figure results from the intersection of

<sup>1</sup>soccer ball (Amer.)

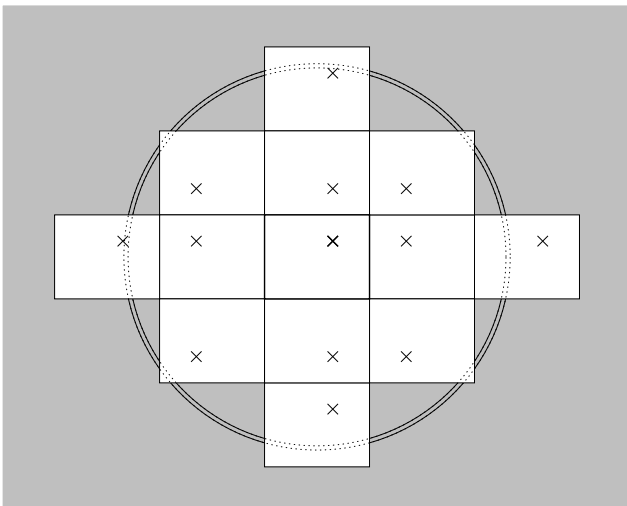


Figure 2: Cross section of the image source space shown in Fig. 1 (white area) with discrete image sources (crosses) and space which should be covered by the late reverberation model (gray area)



Figure 3: Area  $A_m(ct)$  which results from the intersection of the surface of a sphere with the radius  $ct = 10$  m and all image source rooms with an order of 3 or less for a room geometry of  $4.7 \times 4.2 \times 3.2$  m<sup>3</sup>. The ratio of the intersection surface area and the sphere surface area yields the fade-in function  $f(t) = \sqrt{1 - \frac{A_m(ct)}{A(ct)}}$  for the late reverberation tail  $h(t)$ .

the surface of a sphere with the radius  $ct = 10$  m and all image source rooms with an order of 3 or less for a room with the geometry  $4.7 \times 4.2 \times 3.2$  m<sup>3</sup>.

## 2.1. Adjustment of the Intensity Profile

The intensity profile of the late reverberation tail can be adjusted to match the image source model based on the following consideration. Let us assume that the rendering model for the late reverberation is capable of generating a diffuse room impulse response  $\tilde{h}(t)$  containing ideally diffuse late reverberation. An ideally diffuse sound field can be represented by a superposition of travelling plane waves where the phases and propagation directions are a stochastic process [29]. The diffuse room impulse response  $\tilde{h}(t)$  can also be regarded as a superposition of sparse impulse responses  $\tilde{h}_i(t)$  containing the contributions of the plane waves that propagate with directions within a small solid angle. If an audio signal  $s(t)$  is convolved with  $\tilde{h}(t)$ , this can be represented by a superposition of all convolutions of  $s(t)$  with  $\tilde{h}_i(t)$ ,

$$\tilde{y}(t) = s(t) * \sum_i \tilde{h}_i(t) \quad (1)$$

$$= \sum_i s(t) * \tilde{h}_i(t) \quad (2)$$

$$= \sum_i \tilde{y}_i(t) \quad (3)$$

For a diffuse sound field, we can assume that the sparse impulse responses  $\tilde{h}_i(t)$  for disjunct directions are uncorrelated. A convolution of a mono signal with uncorrelated impulse responses decorrelates the signal, and a sum of uncorrelated signals with equal power spectral densities results in a power spectral density which is proportional to the number of signals. By attenuating  $\tilde{y}(t)$  or

$\tilde{h}(t)$  with a gain factor  $\sqrt{\alpha}$  we yield the same power spectral density that can be expected for the case that we take only a portion  $\alpha \in [0, 1]$  of all possible propagation directions into account. In our case, the portion of propagation directions that are taken into account for the late reverberation rendering model is a function of time, quantified by the ratio  $\frac{A_l(ct)}{A(ct)}$ ,

$$\alpha(t) = \frac{A_l(ct)}{A(ct)} = 1 - \frac{A_m(ct)}{A(ct)} . \quad (4)$$

Thus, our fade-in function which adjusts the intensity profile can be specified as follows:

$$f(t) = \sqrt{1 - \frac{A_m(ct)}{A(ct)}} . \quad (5)$$

The reflection density  $D(t)$  in a shoebox room,

$$D(t) = 4\pi \frac{c^3 t^2}{V} , \quad (6)$$

is proportional to the volume  $V(ct)$  of the infinitesimal thin spherical shell [29]. The same applies to the sphere surface  $A(ct)$ . Hence, the ratio  $A_m(ct)/A(ct)$  which results in our fade-in function  $f(t)$  is equal to the ratio of the reflection density  $D_m(t)$  of the image source model and the theoretical reflection density  $D(t)$  in a shoebox room,

$$\frac{A_m(ct)}{A(ct)} = \frac{D_m(t)}{D(t)} . \quad (7)$$

Consequently,  $f(t)$  can also be determined by estimating the reflection density  $D_m(t)$  of the image source model, e.g., by means of a kernel-based smoothing method [30].

## 2.2. Adjustment of the Echo Density Profile

If the late reverberation rendering model synthesizes a room impulse response according to a given echo density profile  $p(t)$ , it can be matched to the rendering parameters of the image source model. A superposition of sparse impulse responses for disjunct directions results in a superposition of their echo density profiles. Thus, we can adjust the echo density profile  $\tilde{p}(t)$  by multiplication with the portion of directions  $\alpha(t)$  that are taken into account at time  $t$ ,

$$p(t) = \left(1 - \frac{A_m(ct)}{A(ct)}\right) \tilde{p}(t) . \quad (8)$$

This adjustment relies on the assumption that the propagation directions are uniformly distributed in a truly diffuse sound field.

## 2.3. Approximation of the Intersection Area

The intersection area  $A_m(ct)$  can be numerically calculated by the sum over all intersection areas  $A_{m,k}(ct)$  where  $k$  denotes the image source room. Each intersection area  $A_{m,k}(ct)$  is delimited by intersection curves which result from the intersection of the surface of the image source room  $k$  and the sphere surface. Each intersection area  $A_{m,k}(ct)$  can then be approximated by triangles as shown in Fig. 3. The accuracy of this approximation method depends on the number of triangles - more triangles result in a higher accuracy but also in a higher computational complexity.

The intersection areas have to be calculated for a great number of discrete points in time to yield the fade-in function  $f(t)$ . We

have developed a fast approximation method for the calculation of the intersection areas  $A_{m,k}(ct)$  to reduce the computational complexity. Instead of approximating the area of convex surfaces by a multitude of triangles, we transform the geometry of the image source rooms so that the intersection area can be approximated by plane areas. This can be achieved by the following steps:

1. Rotate each image source room around the origin so that the center is transformed to the z axis.
2. Replace the z coordinates of the rotated image source room corners by the distance of the corners to the origin.
3. Determine for each distorted image source room the points on the edges of the shoebox room which have the z coordinate  $ct$ . These points define a plane polygon whose area  $\tilde{A}_{m,k}(ct)$  is an approximation for the intersection area  $A_{m,k}(ct)$ .

The first step allows us to approximate the area of the convex intersection surface by the area of a plane polygon which is parallel to the x-y plane. The second step ensures smooth transitions between adjacent image source rooms. The polygon area which is determined in the third step can be calculated using determinants,

$$A_{poly} = \frac{1}{2} \left( \left| \begin{array}{cc} x_n & x_1 \\ y_n & y_1 \end{array} \right| + \sum_{i=1}^{n-1} \left| \begin{array}{cc} x_i & x_{i+1} \\ y_i & y_{i+1} \end{array} \right| \right) , \quad (9)$$

where  $A_{poly}$  is the area of a polygon specified by the corners  $[x_i, y_i]'$ .

The proposed procedure underestimates the area  $A(ct)$  of the sphere surface, because the considered areas are not convex. This deviation can be compensated in first order by an additive constant  $\lambda$ . As  $A_m(ct)$  is only a part of the sphere area, we compensate our estimate  $\tilde{A}_m(ct)$  by adding the compensation offset  $\lambda$  weighted with the area ratio,

$$A_m(ct) \approx \tilde{A}_m(ct) + \lambda \frac{\tilde{A}_m(ct) + \lambda}{A(ct)} . \quad (10)$$

We determine the offset  $\lambda$  by the difference of the exact value  $A(ct_0) = 4\pi(ct_0)^2$  and the estimated value  $\tilde{A}_m(ct_0)$  for the largest radius  $ct_0$  which completely fits into the image source space,

$$\lambda = 4\pi(ct_0)^2 - \tilde{A}_m(ct_0) . \quad (11)$$

This results in  $f(t) = 0$  for  $t = t_0$  which is the actual "starting point" of the fade-in function,

$$f(t) = \begin{cases} 0 & t \leq t_0 \\ \in [0, 1] & \text{else} \end{cases} . \quad (12)$$

Using  $t_0$  for the determination of the offset thus means fulfilling the constraint of an exact solution for  $f(t)$  at the "starting point" of  $f(t)$ . Figure 4 shows a normalized plot of the intersection area  $\tilde{A}_m(ct)$  obtained from our fast approximation procedure, a normalized plot of the sphere surface  $A(ct)$  to illustrate the offset  $\lambda$ , the resulting fade-in function  $f(t)$ , and the deviation from the fade-in function  $f_{\Delta}(t)$  obtained from the triangle approximation method. We observe that the difference of the resulting fade-in functions is neglectable small.

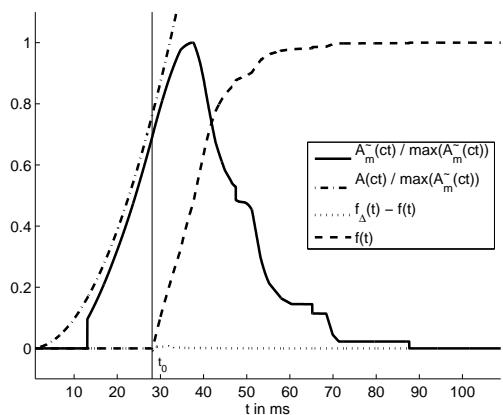


Figure 4: Normalized plot of the intersection area  $\tilde{A}_m(ct)$  for a  $6.65 \times 4.90 \times 3.50 \text{ m}^3$  room obtained from the fast approximation method for image sources up to the fourth order; normalized plot of the sphere surface  $A(ct)$ , resulting fade-in function  $f(t)$ , and deviation from the fade-in function  $f_{\Delta}(t)$  obtained from the triangle approximation method

### 3. SYNTHESIS OF LATE REVERBERATION

The adjustment methods for the late reverberation described in Sec. 2.1 and Sec. 2.2 can easily be implemented with a statistical time-frequency model. Moorer suggested to use a random noise signal attenuated by a frequency dependent exponential decay for the synthesis of an artificial late reverberation tail [20]. The adjustment of the intensity profile using a fade-in function  $f(t)$  for such a model is shown in Fig. 5. The echo density profile can be taken into account for a discrete noise signal by thinning out the random noise signal  $g(n)$  to a desired density  $p(n)$  [3],

$$s(n) = \begin{cases} g(n) & u(n) \leq p(n)/f_s \\ 0 & \text{else} \end{cases}, \quad (13)$$

where  $s(n)$  is a sparse version of the noise signal at the sampling frequency  $f_s$  using an additional random signal  $u(n)$  which is uniformly distributed between 0 and 1.

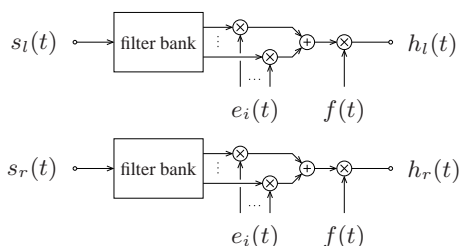


Figure 5: Generation of an artificial binaural late reverberation tail  $h_l(t)$  and  $h_r(t)$  from uncorrelated white noise  $s_l(t)$  and  $s_r(t)$ ; the frequency-dependent reverberation time is adjusted by the exponential decay  $e_i(t)$  in frequency band  $i$ ; the fade-in function  $f(t)$  is used for a smooth combination with the early reflection model

### 4. INFORMAL LISTENING TEST

In order to evaluate our proposed method, we conducted informal listening tests with audio examples which differ only by the used fade-in function as shown in Fig. 6. In addition to our proposed fade-in function, we used a linear fade-in function as applied by Braasch [31], and a step function which emulates an artificial reverberator with a pre-delay. For the pre-delay  $t_{step}$ , we used the mean of the starting point  $t_0$  and the end point  $t_1$  of our proposed fade-in function. The four selected listeners (“A”, “B”, “C”, and “D”) play at least one musical instrument and have experience with artificial reverberators. All listeners are between 25 and 35 years old and are normally-hearing as verified recently by an audiogram. We asked them to rate the naturalness of the stimuli on a scale between 0 (“bad”) and 100 (“excellent”). We selected two virtual rooms with different reverberation times (a small hall with  $T_{60} = 1.4 \text{ s}$  and a large hall with  $T_{60} = 1.8 \text{ s}$ ) for our test. As stimuli, we chose two pieces of music, a soft piano improvisation and a Jazz tune which also includes drums (“Cantaloupe Island”, Herbie Hancock). The listening test was conducted using four Genelec 2029BL loudspeakers in 1.3 m distance at  $\pm 30^\circ$  and  $\pm 110^\circ$ . Table 1 lists the ratings of the test listeners, the mean value  $\mu$ , and the standard deviation  $\sigma$ .

### 5. DISCUSSION AND FUTURE WORK

The listeners of the informal listening test reported that they were able to detect the acoustical defect caused by the gap in the impulse response of the “pre-delay” stimulus. In three out of the

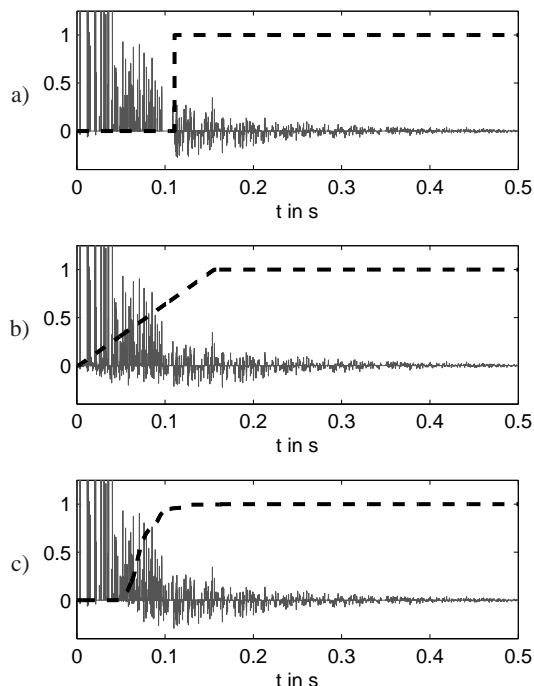


Figure 6: Fade-in functions (dashed) used for the informal listening test; the room impulse responses (solid, gray) were synthesized for a multi-speaker setup as described in [3, 24]; a) step function, b) linear function, c) result of the proposed method

room	music	fade-in function	“A”	“B”	“C”	“D”	$\mu$	$\sigma$
small hall	piano only	pre-delay	85	50	80	50	66.25	18.87
small hall	piano only	linear	87	85	80	50	75.5	17.25
small hall	piano only	proposed method	86	70	80	90	81.5	8.70
small hall	piano + drums	pre-delay	86	60	70	85	75.25	12.53
small hall	piano + drums	linear	88	60	70	85	75.75	13.12
small hall	piano + drums	proposed method	90	80	70	70	77.5	9.57
large hall	piano only	pre-delay	84	35	85	70	68.5	23.36
large hall	piano only	linear	87	10	90	70	64.25	37.22
large hall	piano only	proposed method	86	40	90	95	77.75	25.43
large hall	piano + drums	pre-delay	86	50	75	70	70.25	15.06
large hall	piano + drums	linear	86	60	80	80	76.5	11.36
large hall	piano + drums	proposed method	86	45	80	60	67.75	18.80

Table 1: Naturalness as rated by four selected listeners (“A”, “B”, “C”, and “D”), mean  $\mu$ , and standard deviation  $\sigma$  for two simulated rooms of different size and two different stimuli

four selected scenarios, the stimulus based on our proposed fade-in function got the highest mean rating. However, due to the overlapping confidence intervals of the test results (e.g.,  $2\sigma$  for a 95% confidence interval), this preference is not statistical significant. In reverse, there is no evidence, that our proposed combination method is significantly worse than previously used methods. As our method relies on a solid theoretical foundation, we have good reasons to prefer it over the other methods.

As the fade-in function  $f(t)$  is applied to a randomly generated impulse response, we can assume that a deviation from the exact solution is tolerable to some extent. Thus, we can sub-sample and interpolate the fade-in function  $f(t)$  between the “starting point”  $t_0$  and the “end point”  $t_1$  to further reduce the computational complexity for the determination of an approximated version of  $f(t)$ . E.g., for a shoebox room of the ratio 1.9 : 1.4 : 1.0 and specular reflections up to the fourth order, using 100 sample points provides a sufficient accuracy and requires less than one second calculation time on a current PC (0.16 s with our C++ implementation and 0.82 s with our Matlab implementation on a PC with a 2.1 GHz Core2 Duo processor).

A shoebox shaped room results in a quite simple solution for an optimal combination method due to its simple geometry. Even though a shoebox geometry is sufficient for applications where no specific room geometry is required, this is a clear restriction. For those cases where a shoebox geometry is not applicable, the intersection principle discussed in this paper could be applied to arbitrary geometries based on a beam-tracing algorithm where the visible parts of the image source rooms are constructed from the beams.

The presented combination method ensures that the late reverberation model takes over the part which is not covered by the early reflection model. Even though this results in a smooth transition, this constitutes a model which simulates either specular or diffuse reflections. A more realistic result could be achieved by also adding portions of diffuse reverberation to specular reflections. The amount of diffuse reverberation can be determined from the absorption coefficients as proposed by Kuttruff [32]. By disassembling the intersection area  $A_m(ct)$  into areas  $S_n(ct)$  which belong to image source rooms of a certain order  $n$ ,

$$A_m(ct) = \sum_{n=0}^N S_n(ct) \quad , \quad (14)$$

we have detailed information about the contributions of the reflections of a certain order at a given time  $t$ . From a weighted sum of the contributing portions, we can derive a fade-in function  $f_d(t)$  in addition to  $f(t)$  which adds portions of diffuse reverberation to the specular reflections. In *tinyAVE* we have implemented the approximation method described in Sec. 2.3 by a loop over all image source rooms  $k$  and by summing up the intersection areas  $A_{m,k}(ct)$ . Instead of summing up  $A_{m,k}(ct)$  to a single vector  $A_m(ct)$ , we could compute a set of vectors  $S_n(ct)$  by adding  $A_{m,k}(ct)$  to  $S_{n(k)}(ct)$  in our loop. This would not even increase the computational complexity.

## 6. CONCLUSIONS

We proposed a new method for matching a late reverberation model and an image source model for shoebox shaped rooms. This allows the diffuse late reverberation to be matched to the early specular reflections with regard to the parameters of the image source model. In our approach, we also take the room extension in all three dimensions into account. If one room dimension is significantly larger or smaller than the others, the rendering models are combined accordingly.

We presented two possible adjustment methods for matching the late reverberation tail, i.e. by adjusting the intensity profile or by adjusting the echo density profile. We showed how the adjustment functions for these profiles can be derived from the intersection of the space covered by the image source model and a sphere surface and how it can be included into a statistical time-frequency late reverberation model.

Furthermore, we presented a computational efficient method for the approximation of the above mentioned intersection area. We showed that our approximation results in neglectable small deviations for the resulting fade-in function. We showed how the computational complexity can be further reduced by sub-sampling and interpolation. An interpolated version of the fade-in function which provides sufficient accuracy can be determined in less than one second calculation time on a current PC.

In an informal listening test with four expert listeners we observed that our proposed combination method got the highest mean rating in three out of four scenarios. Even though this is not statistical significant, there is evidence that our proposed method is in terms of naturalness at least comparable to previously applied

methods. As our method relies on a solid theoretical foundation, it is our preferred method.

## 7. REFERENCES

- [1] J.-M. Jot and O. Warusfel, "A Real-Time Spatial Sound Processor for Music and Virtual Reality Applications," in *International Computer Music Conference*, Banff, Canada, 1995.
- [2] A. Silzle, P. Novo, and H. Strauss, "IKA-SIM: A System to Generate Auditory Virtual Environments," in *116th AES Convention*, Berlin, Germany, 2004.
- [3] C. Borß and R. Martin, "An Improved Parametric Model for Perception-Based Design of Virtual Acoustics," in *AES 35th Int. Conference*, London, UK, Feb. 2009.
- [4] Vorländer, M., "International round Robin on room acoustical computer simulations," in *Proc. 15th International Congress on Acoustics (ICA)*, Trondheim, Norway, 1995, pp. 689–692.
- [5] A. Krokstad and S. Strom, and S. Sorsdal, "Calculating the Acoustical Room Response by the Use of a Ray Tracing Technique," *J. Sound Vib.*, vol. 8, no. 1, pp. 118–125, 1968.
- [6] J. P. Walsh, "The Design of Godot: A System for Room Acoustics Modeling and Simulation," in *10th Int. Congr. on Acoustics*, Sydney, Australia, 1980.
- [7] D. van Maercke, "Simulation of Sound Fields in Time and Frequency Domain Using a Geometrical Model," in *12th Int. Congr. on Acoustics*, Toronto, Canada, 1986.
- [8] G. M. Naylor, "ODEON - another hybrid room acoustical model," *Applied Acoustics*, vol. 38, no. 2-4, pp. 131–143, 1993.
- [9] W. Ahnert and R. Feistel, "EARS Auralization Software by Ahnert," *J. Audio Eng. Soc.*, vol. 41, no. 11, pp. 894–904, 1993.
- [10] B.-I. L. Dalenbäck, "Verification of Prediction Based on Randomized Tail-Corrected Cone-Tracing and Array Modeling," *J. Acoust. Soc. Am.*, vol. 105, no. 2, pp. 1173, Feb. 1999.
- [11] T. Funkhouser et al., "A Beam Tracing Method for Interactive Architectural Acoustics," *J. Acoust. Soc. Am.*, vol. 115, no. 2, pp. 739–756, Feb. 2004.
- [12] T. Lentz and D. Schröder and M. Vorländer and I. Assenmacher, "Virtual Reality System with Integrated Sound Field Simulation and Reproduction," *EURASIP Journal on Advances in Signal Processing*, vol. 2007, 2007, Article ID 70540.
- [13] T. Lewers, "A Combined Beam Tracing and Radiant Exchange Computer Model of Room Acoustics," *Applied Acoustics*, vol. 38, pp. 161–178, 1993.
- [14] B.-I. L. Dalenbäck, "Room Acoustic Prediction Based on a Unified Treatment of Diffuse and Specular Reflection," *J. Acoust. Soc. Am.*, vol. 100, no. 2, pp. 899–909, 1996.
- [15] J.B. Allen and D.A. Berkley, "Image method for efficiently simulating small-room acoustics," *J. Acoust. Soc. Am.*, vol. 65, no. 4, pp. 943–950, 1979.
- [16] Vorländer, M., "Simulation of the Transient and Steady-State Sound Propagation in Rooms Using a New Combined Ray-Tracing/Image-Source Algorithm," *J. Acoust. Soc. Am.*, vol. 86, no. 1, pp. 172–178, Jul. 1989.
- [17] J. Jot, "Efficient Models for Reverberation and Distance Rendering in Computer Music and Virtual Audio Reality," in *International Computer Music Conference*, 1997.
- [18] L. Savioja et al., "Creating Interactive Virtual Acoustic Environments," *Journal of the Audio Engineering Society*, vol. 47, no. 9, pp. 675–705, Sep. 1999.
- [19] M. R. Schroeder, "Natural Sounding Artificial Reverberation," *Journal of the Audio Engineering Society*, vol. 10, no. 3, pp. 219–223, 1962.
- [20] J. Moorer, "About this Reverberation Business," *Computer Music Journal*, vol. 3, no. 2, pp. 13–18, 1979.
- [21] R. Väänänen et al., "Efficient and Parametric Reverberator for Room Acoustics Modeling," in *International Computer Music Conference (ICMC '97)*, Thessaloniki, Greece, Sep. 1997.
- [22] W. G. Gardner, "A Realtime Multichannel Room Simulator," in *124th Meeting of the Acoustical Society of America*, New Orleans, LA, USA, Nov. 1992.
- [23] J. Stautner and M. Puckette, "Designing Multi-Channel Reverberators," *Computer Music J.*, vol. 6, no. 1, pp. 52–65, 1982.
- [24] C. Borß, "A VST Reverberation Effect Plugin Based on Synthetic Room Impulse Responses," in *12th Int. Conference on Digital Audio Effects (DAFx-09)*, Como, Italy, Sep. 2009, (accepted for publication).
- [25] J.-M. Jot and L. Cerveau and O. Warusfel, "Analysis and Synthesis of Room Reverberation Based on a Statistical Time-Frequency Model," in *103rd AES Convention*, New York, NY, USA, 1997.
- [26] K. Meesawat and D. Hammershøi, "An Investigation on the Transition from Early Reflections to a Reverberation Tail in a BRIR," in *International Conference on Auditory Display*, Kyoto, Japan, Jul. 2002.
- [27] K. Meesawat and D. Hammershøi, "The Time When the Reverberation Tail in a Binaural Room Impulse Response Begins," in *115th AES Convention*, New York, NY, USA, Oct. 2003.
- [28] C. Borß, "Audio examples rendered with tinyAVE," 2009, URL: [http://www2.ika.rub.de/tinyAVE\\_orchestra/](http://www2.ika.rub.de/tinyAVE_orchestra/).
- [29] H. Kuttruff, *Room Acoustics*, Applied Sci. Publrs., Essex, England, first edition, 1973.
- [30] A. W. Bowman and A. Azzalini, *Applied Smoothing Techniques for Data Analysis*, Oxford University Press, 1997.
- [31] J. Braasch, "Cranial Transitions for Soprano Saxophone and Electronic Processing," in *13th Int. Conf. on Auditory Display*, Montreal, Canada, June 2007, pp. 60–67.
- [32] H. Kuttruff, "A Simple Iteration Scheme for the Computation of Decay Constants in Enclosures with Diffusely Reflecting Boundaries," *J. Acoust. Soc. Am.*, vol. 98, no. 1, pp. 288–293, 1995.